# Mechanism of Heat Transfer Enhancement in Recuperators with Oblique Wavy Walls*

Kenichi MORIMOTO†, Yuji SUZUKI†, and Nobuhide KASAGI†

**Key Words:** *Recuperator, Direct Numerical Simulation, Heat Transfer Enhancement*

## 1 Introduction

Small-scale distributed energy systems with micro gas turbines are of great concern because of their high efficiency and low environmental impact. It is pointed out that one of the most important technical issues to improve the system efficiency is the effectiveness of recuperators [1].

Recently, primary surface recuperators have been considered promising and employed in recuperated turbine systems [2]. We report that the appropriate use of oblique wavy walls in counter flow recuperators can induce intense secondary flows and realize significant heat transfer enhancement at the cost of relatively small pressure loss [3].

In the present study, the detailed mechanism of heat transfer enhancement is investigated in order to obtain a clue to optimal shape design of the passage geometry. We focus on the coupling effects of counter-flowing fluids on local heat transfer characteristics.

## 2 Numerical Procedures

Figure 1 shows the coordinate system and passage geometry considered in this study. Surface shapes of the top and bottom walls are defined as follows:

$$y_{w,top} = y_{w,bottom} = A\cos 2\pi/L_x\,(x - z\tan\gamma), \qquad (1)$$

where $L_x$ and $\gamma$ (= $\tan^{-1}(L_x/2\pi)$) denote the streamwise pitch and oblique angle of wavy surfaces, respectively. Two types of heat exchanger configurations with staggered arrangement of hot and cold fluids are examined as shown in Fig. 2. Each passage is surrounded by oblique wavy walls (top and bottom walls) and flat side walls (left and right walls). Thermal resistance of the dividing walls is neglected. The oblique angles of adjacent passages in Case 1 are the same in the $z$-direction, while those in Case 2 are opposite in sign. The working fluids are air, and the bulk mean temperature is kept constant at each inlet. The Reynolds number Re based on the bulk mean streamwise velocity $U_b$ and the hydraulic diameter $D_h$ is set constant at about 200. Periodic boundary condition is imposed in the $x$-direction. For the thermal boundary condition, temperature and heat fluxes are assumed to be the same on both sides of the dividing walls [3].

## 3 Results and Discussion

Figure 3 shows the $j/f$ factor normalized with that in straight square ducts versus the oblique angles $\gamma$. Wave amplitude $A$ is kept constant at $0.20\pi$. Results under isothermal heated conditions are also plotted for comparison. Heat transfer enhancement in the present passage becomes larger than the pressure loss penalty, and the $j/f$ factor is maximized at $\gamma \sim 60°$ in Case 2 [3]. The sum of the heat fluxes on the wavy top and bottom walls has larger contribution to the total heat transfer than that on the side walls. Hereafter, the mechanism of heat transfer enhancement on the wavy walls is discussed in detail.

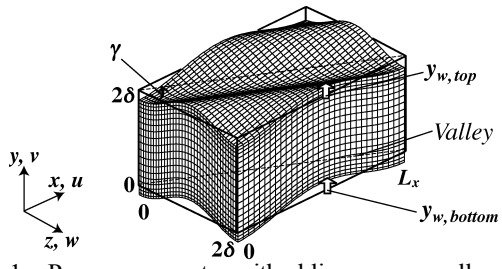


Fig. 1 Passage geometry with oblique wavy walls.

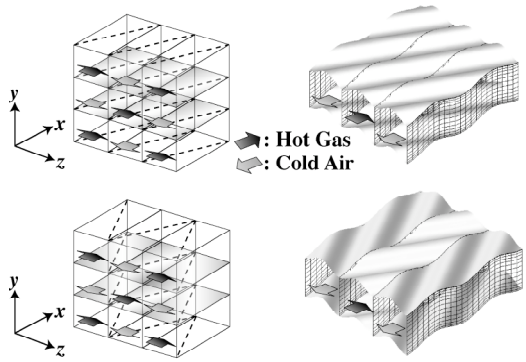


Fig. 2 Configurations of modeled counter-flow heat exchangers: (a) Case 1, (b) Case 2.

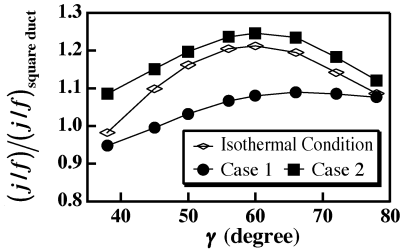


Fig. 3 Effect of oblique angles on $j/f$ factors.

Figure 4 shows the shear stress vectors on the bottom wall, projected onto the $x$-$z$ plane. The oblique wavy wall induces a flow along the valley (A) and a flow over the hill toward the left wall (B). The size of the flow separation

Received : July , 2004, Editor :

† Department of Mechanical Engineering, The University of Tokyo (7-3-1 Hongo, Bunkyo-ku, Tokyo, 113-8656, JAPAN)

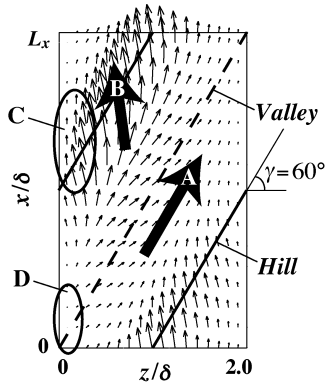


Fig. 4 Wall shear stress vectors projected onto the *x*-*z* plane.

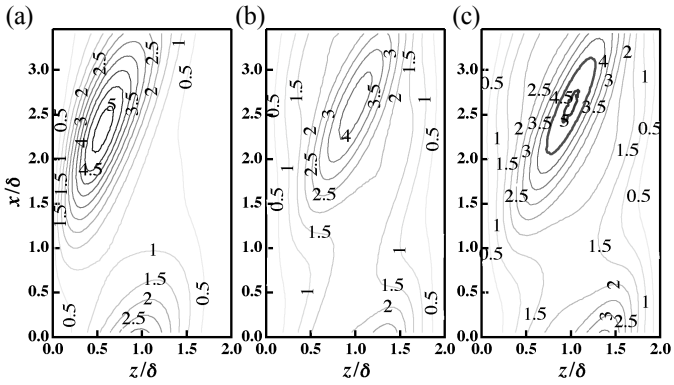


Fig. 5 Wall heat flux distributions under different thermal boundary conditions: (a) Isothermal heated condition, (b) Coupling condition (Case 1), (c) Coupling condition (Case 2).

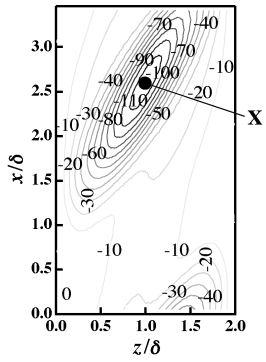


Fig.6 Inner product of the wall shear stress vectors.

bubble (D) is dependent on the magnitude of the flow over the hill near the left wall (C). At $\gamma$= 60°, the heat transfer is markedly augmented by the strong secondary flow, of which magnitude reaches up to 20% of the bulk mean velocity, while the flow separation is minimized. Therefore, the *j/f* factor takes its maximum value. Heat flux distributions on the bottom wall under different thermal boundary conditions are shown in Fig. 5. Whereas distributions of the wall heat fluxes and the wall shear stresses exhibit similar patterns in the isothermal conditions, the heat flux distributions in Cases 1 and 2 change their profiles due to the thermal coupling effect of the fluid motions on both sides of the wall. In the isothermal case, heat flux near the right wall remains small, because the streamwise flow velocity is small near the wall. On the other hand, heat flux is markedly increased for the coupling conditions. The flow arrangement of Case 2 enhances the thermal coupling effect larger than that of Case 1, because of the high-speed fluid in the adjacent flow passages surrounding the right wall. The dissimilarity between the velocity and temperature fields near the walls is more significant in Case 2 than in Case 1.

Figure 6 shows distribution of the inner product of the wall shear stress vectors ($\vec{\tau}_{w,h}$: hot side, $\vec{\tau}_{w,c}$: cold side) acting on both sides of the bottom wall. The peak locates at the point X ((*x*, *y*, *z*) = (3/4 $L_x$, 0, 1.0$\delta$)), where $\vec{\tau}_{w,c}$ = $\delta\vec{\tau}_{w,h}$ due to the flow symmetry. It is observed that the distribution of the inner product corresponds well to the heat flux distribution in the thermal coupling conditions. Figure 7 shows the wall-averaged inner product and product of magnitudes of the wall shear stress vectors. The quantities are normalized with those of the analytical solution in straight square ducts. It can be seen that the inner product takes its maximum value at $\gamma$~ 60° and its behavior is in agreement with that of the *j/f* factor. The product of the magnitudes, on the other hand, is maximized at $\gamma$~ 50°, which corresponds to the trend of the averaged Nusselt number. This is because the absolute value of the shear stress vectors becomes largest at $\gamma$~ 50°, but the inner product is reduced due to the reverse flow associated with the flow separation. Therefore, the inner product can

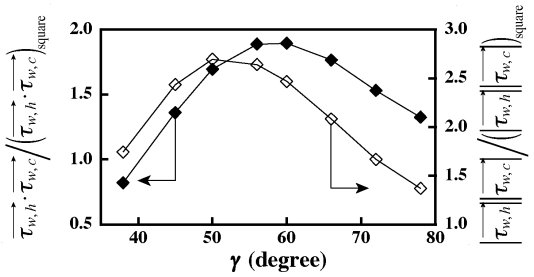


Fig. 7 Wall-averaged values of the inner product and product of magnitudes of the wall shear stress vectors versus the oblique angle.

account for the increase of pressure loss with separation, and is a good indicator for the *j/f* factor.

## 4 Concluding Remarks

Heat transfer and pressure loss characteristics of modeled counter-flow recuperators with oblique wavy walls are examined using direct numerical simulation, and the detailed mechanism of heat transfer enhancement is investigated. When thermal coupling of adjacent counter flows is considered, the characteristic of the *j/f* factor is found to be closely related to the inner product of the wall shear stress vectors acting on both sides of the wavy wall. This correlation is expected to be a clue toward optimal shape design of the heat exchanger passage, in which the thermal coupling is crucial to the heat transfer performance.

**Acknowledgements**

This work was supported by a CREST project of the Japan Science and Technology Agency (JST), and by the Grant-in-Aid for JSPS Fellows (No. 15-11654) of the Ministry of Education, Culture, Sports, Science and Technology of Japan (MEXT).

**References**

[1] Kasagi, N., and Kimijima, S., *Energy and Resources*, **23**-3, (2002), 183, (in Japanese).
[2] McDonald, C. F., *Appl. Therm. Eng.*, **20**-5, (2000), 471.
[3] Morimoto, K., Suzuki, Y., and Kasagi, N., *Proc. Therm. Eng. Conf.*, **03**-30, (2003), 445, (in Japanese).